

# The Straight-Line RAC Drawing Problem Is NP-Hard\*

Evmorfia N. Argyriou, Michael A. Bekos, and Antonios Symvonis

School of Applied Mathematical & Physical Sciences,  
National Technical University of Athens, Greece  
{fargyriou,mikebekos,symvonis}@math.ntua.gr

**Abstract.** Recent cognitive experiments have shown that the negative impact of an edge crossing on the human understanding of a graph drawing, tends to be eliminated in the case where the crossing angles are greater than 70 degrees. This motivated the study of *RAC drawings*, in which every pair of crossing edges intersects at right angle. In this work, we demonstrate a class of graphs with unique RAC combinatorial embedding and we employ members of this class in order to show that it is  $\mathcal{NP}$ -hard to decide whether a graph admits a straight-line RAC drawing.

## 1 Introduction

In the graph drawing literature, the problem of finding aesthetically pleasant drawings of graphs has been extensively studied. The graph drawing community has introduced and studied several criteria that judge the quality of a graph drawing, such as the number of crossings among pairs of edges, the number of edge bends, the maximum edge length, the total area occupied by the drawing and so on (see the books [5,17]).

Motivated by the fact that the edge crossings have negative impact on the human understanding of a graph drawing [20], a great amount of research effort has been devoted on the problem of finding drawings with minimum number of edge crossings. Unfortunately, this problem is  $\mathcal{NP}$ -complete in general [12]. However, recent eye-tracking experiments by Huang et al. [15,16] indicate that the negative impact of an edge crossing is eliminated in the case where the crossing angle is greater than 70 degrees. These results motivated the study of a new class of drawings, called *right-angle drawings* or *RAC drawings* for short [1,7,8,9]. A RAC drawing of a graph is a polyline drawing in which every pair of crossing edges intersects at right angle.

Didimo, Eades and Liota [8] proved that it is always feasible to construct a RAC drawing of a given graph with at most three bends per edge. In this work, we prove that the problem of determining whether an input graph admits a straight-line RAC drawing is  $\mathcal{NP}$ -hard.

---

\* Funded by the Operational Programme on Education and Lifelong Learning (Action Hrakleitios-II) which is co-financed by Greece and the European Union (European Social Fund NSRF 2007-2013).

## 1.1 Related Work

Didimo et al. [8] initiated the study of RAC drawings and showed that any straight-line RAC drawing with  $n$  vertices has at most  $4n - 10$  edges and that any graph admits a RAC drawing with at most three bends per edge. Angelini et al. [1] showed that the problem of determining whether an acyclic planar digraph admits a straight-line upward RAC drawing is  $\mathcal{NP}$ -hard. Furthermore, they constructed digraphs admitting straight-line upward RAC drawings, that require exponential area. Di Giacomo et al. [7] studied the interplay between the crossing resolution, the maximum number of bends per edges and the required area. Didimo et al. [9] presented a characterization of complete bipartite graphs that admit a straight-line RAC drawing. Arikushi et al. [4] studied polyline RAC drawings in which each edge has at most one or two bends and proved that the number of edges is at most  $O(n)$  and  $O(n \log^2 n)$ , respectively. Dujmovic et al. [10] studied  $\alpha$  *Angle Crossing* (or  $\alpha AC$  for short) drawings, i.e., drawings in which the smallest angle formed by an edge crossing is at least  $\alpha$ . In their work, they presented upper and lower bounds on the number of edges. Van Kreveld [18] showed that the quality of a planar drawing of a planar graph, evaluated in terms of area required, edge-length and angular resolution, can be improved if one allows right-angle crossings.

Closely related to the RAC drawing problem, is the angular resolution maximization problem, i.e., the problem of maximizing the smallest angle formed by any two adjacent edges. Note that both problems correlate the resolution of a graph with the visual distinctiveness of the edges in a graph drawing. Formann et al. [11] introduced the notion of the angular resolution of straight-line drawings. In their work, they proved that determining whether a graph of maximum degree  $d$  admits a drawing of angular resolution  $\frac{2\pi}{d}$  (i.e., the obvious upper bound) is  $\mathcal{NP}$ -hard. They also presented upper and lower bounds on the angular resolution for several types of graphs of maximum degree  $d$ . Malitz and Papakostas [19] proved that for any planar graph of maximum degree  $d$ , it is possible to construct a planar straight-line drawing with angular resolution  $\Omega(\frac{1}{7d})$ . Garg and Tamassia [13] presented a continuous tradeoff between the area and the angular resolution of planar straight-line drawings. For the case of connected planar graphs with  $n$  vertices and maximum degree  $d$ , Gutwenger and Mutzel [14] presented a linear time algorithm that constructs planar polyline grid drawings on a  $(2n - 5) \times (\frac{3}{2}n - \frac{7}{2})$  grid with at most  $5n - 15$  bends and minimum angle greater than  $\frac{2}{d}$ . Bodlaender and Tel [6] showed that planar graphs with angular resolution at least  $\frac{\pi}{2}$  are rectilinear. Argyriou et al. [2] studied a generalization of the crossing and angular resolution maximization problems, in which the minimum of these quantities is maximized and presented optimal algorithms for complete graphs and a force-directed algorithm for general graphs.

The rest of this paper is structured as follows: In Section 2, we introduce preliminary properties and notation. In Section 3, we present a class of graphs with unique RAC combinatorial embedding. In Section 4, we show that the straight-line RAC drawing problem is  $\mathcal{NP}$ -hard. We conclude in Section 5 with open problems.

## 2 Preliminaries

Let  $G = (V, E)$  be a simple, undirected graph drawn in the plane. We denote by  $\Gamma(G)$  the drawing of  $G$ . The following properties are used in the rest of this paper.

*Property 1 (Didimo, Eades and Liota [8]).* In a straight-line RAC drawing there cannot be three mutually crossing edges.

*Property 2 (Didimo, Eades and Liota [8]).* In a straight-line RAC drawing there cannot be a triangle  $\mathcal{T}$  and two edges  $(a, b)$  and  $(a, b')$ , such that  $a$  lies outside  $\mathcal{T}$  and  $b, b'$  lie inside  $\mathcal{T}$ .

## 3 A Class of Graphs with Unique RAC Combinatorial Embedding

The  $\mathcal{NP}$ -hardness proof employs a reduction from the well-known 3-SAT problem. However, before we proceed with the reduction details, we first provide a graph, referred to as *augmented square antiprism graph*, which has the following property: All RAC drawings of this graph have two “symmetric” combinatorial embeddings. Figures 1a and 1b illustrate this property. Observe that the augmented square antiprism graph consists of a “central” vertex  $v_0$ , which is incident to all vertices of the graph, and two quadrilaterals (refer to the dashed and bold drawn squares in Figure 1b), that are denoted by  $\mathcal{Q}_1$  and  $\mathcal{Q}_2$  in the remainder of this paper. Removing the central vertex, the remaining graph corresponds to the skeleton of a square antiprism, and, it is commonly referred to as *square antiprism graph*.

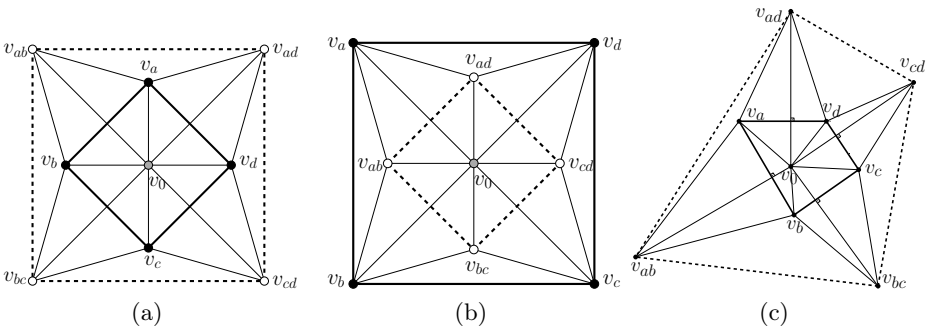


**Fig. 1.** (a)-(b) Two different RAC drawings of the augmented square antiprism graph with different combinatorial embeddings. (a)-(c) Two different RAC drawings with the same combinatorial embedding

If we replace the two quadrilaterals with two triangles, then the implied graph is the *augmented triangular antiprism graph*. Didimo et al. [8], who showed that any  $n$ -vertex graph which admits a RAC-drawing can have at most  $4n - 10$  edges,

used the augmented triangular antiprism graph, as an example of a graph that achieves the bound of  $4n - 10$  edges (see Figure 1c in [8]). In contrast to the augmented triangular antiprism graph, the augmented square antiprism graph does not achieve this upper bound. In general, the class of *the augmented  $k$ -gon antiprism graphs*,  $k \geq 3$ , is a class of non-planar graphs, that all admit RAC drawings. Recall that any planar  $n$ -vertices graph, should have  $3n - 6$  edges, and since an augmented  $k$ -gon antiprism graph has  $2k + 1$  vertices and  $5k$  edges, it is not planar for the entire class of these graphs.

**Theorem 1.** *Any straight-line RAC drawing of the augmented square antiprism graph has two combinatorial embeddings.*

*Sketch of proof.* The proof of this theorem is implied by the following properties:

- *Property A:* There does not exist a RAC drawing of the augmented square antiprism graph in which the central vertex  $v_0$  lies on the exterior of quadrilateral  $Q_i$ ,  $i = 1, 2$ , and an edge connecting  $v_0$  with a vertex of  $Q_i$  crosses an edge of  $Q_i$ .
- *Property B:* In any RAC drawing of the augmented square antiprism graph, quadrilateral  $Q_i$ ,  $i = 1, 2$ , is drawn planar.
- *Property C:* In any RAC drawing of the augmented square antiprism graph, the central vertex  $v_0$  lies in the interior of quadrilateral  $Q_i$ ,  $i = 1, 2$ .
- *Property D:* There does not exist a RAC drawing of the augmented square antiprism graph where an edge emanating from vertex  $v_0$  towards a vertex of quadrilateral  $Q_i$ ,  $i = 1, 2$ , crosses quadrilateral  $Q_i$ .
- *Property E:* There does not exist a RAC drawing of the augmented square antiprism graph in which quadrilateral  $Q_1$  intersects  $Q_2$ .

Due to space constraints, the proofs of these properties are omitted. The proofs make use of elementary geometric properties, they heavily use Properties 1 and 2, and are based on exhaustive cases analysis on the relative positions of (a) the central vertex  $v_0$ , and, (b) quadrilaterals  $Q_1$  and  $Q_2$ . For more details, we refer the reader to [3].  $\square$

We extend the augmented square antiprism graph, by appropriately “glueing” multiple instances of it, the one next to the other, either horizontally or vertically. Figure 2a demonstrates how a horizontal extension of two instances, say  $G$  and  $G'$ , is realized, i.e., by identifying two “external” vertices, say  $v$  and  $v'$ , of  $G$  with two “external” vertices of  $G'$  (refer to the gray-colored vertices of Figure 2a), and by employing an additional edge (refer to the dashed drawn edge of Figure 2a), which connects an “internal” vertex, say  $u$ , of  $G$  with the corresponding “internal” vertex, say  $u'$ , of  $G'$ . Let  $G \oplus G'$  be the graph produced by a horizontal or vertical extension of  $G$  and  $G'$ . Since each of  $G$  and  $G'$  has two RAC combinatorial embeddings each, one would expect that  $G \oplus G'$  would have four possible RAC combinatorial embeddings. We will show that this is not true and, more precisely, that there only exists a single RAC combinatorial embedding.

**Theorem 2.** *Let  $G$  and  $G'$  be two instances of the augmented square antiprism graph. Then,  $G \oplus G'$  has a unique RAC combinatorial embedding.*

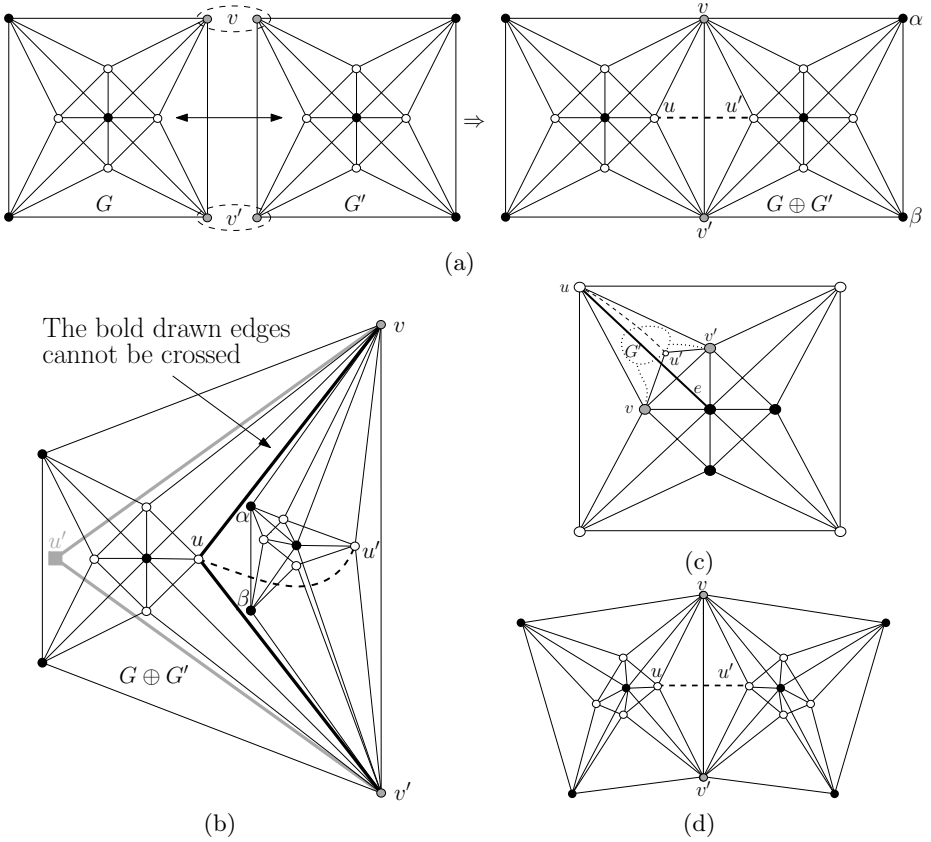


**Fig. 2.** (a) Horizontal extension of two instances of the augmented square antiprism graph, (b) The additional (dashed) edge does not permit the second instance to be drawn in the interior of the first one. (c) The vertices which are identified, during a horizontal or vertical extension ( $v$  and  $v'$  in Figure), should be on the external face of each augmented square antiprism graph. (d) At each extension step the new instance of the augmented square antiprism graph may introduce a “turn”.

*Proof.* Assume first that in a RAC drawing of  $G \oplus G'$ , vertices  $v$  and  $v'$  are on the external quadrilateral of  $G$  and graph  $G'$  is drawn completely in the interior of  $G$  (see Figure 2b; since  $v$  and  $v'$  are on the external face of  $G'$ , vertices  $\alpha$  and  $\beta$  in Figure 2b should also be on the external face of  $G'$ ). First observe that vertex  $u'$  of  $G'$ , which is incident to vertices  $v$  and  $v'$ , cannot reside to the “left” of both edges  $(u, v)$  and  $(u, v')$  (refer to the bold drawn edges of Figure 2b), since this would lead to a situation where three edges mutually cross and, subsequently, to a violation of Property 1 (see the gray-colored square vertex of Figure 2b). Therefore, vertex  $u'$  should lie within the triangular face of  $G$  formed by vertices  $u, v$  and  $v'$ . The same similarly holds for the central vertex of  $G'$ , which is also incident to vertices  $v$  and  $v'$ . By Property 2, any common neighbor of vertices  $u'$  and  $v$  should also lie within the same triangular face of  $G$ , which progressively

implies that entire graph  $G'$  should reside within this face, as in Figure 2b. However, in this case and since  $u'$  is incident to  $v$  and  $v'$ , edge  $(u, u')$ , which is used on a horizontal or a vertical extension, crosses the interior of  $G'$ , which is not permitted. This suggests that graph  $G'$  should be on the exterior of  $G$ .

Now assume that vertices  $v$  and  $v'$ , which are identified, during a horizontal or vertical extension, are along the internal quadrilateral of  $G$  in a RAC drawing of  $G \oplus G'$ . This is illustrated in Figure 2c. Then, the edge, say  $e$ , which perpendicularly crosses edge  $(v, v')$  and emanates from the external quadrilateral towards the central vertex of  $G$  (refer to the bold solid edge of Figure 2c) will be involved in crossings with  $G'$ . More precisely, we focus on vertex  $u'$  of  $G'$ , which is incident to vertices  $v$  and  $v'$ . These edges will inevitably introduce non-right angle crossings, since one of them should cross edge  $e$ . Therefore, the vertices that are identified, during a horizontal or vertical extension, should always be on the external face of each augmented square antiprism graph and, subsequently, the drawing of the graph produced by a horizontal or vertical extension will resemble the one of Figure 2a, i.e., it has a unique embedding.  $\square$

Note that the extension which is given in Figure 2a, is ideal. In the general case, at each extension step the new instance of the augmented square antiprism graph may introduce a “turn”, as in Figure 2d. We observe that by “glueing” a new instance of the augmented square antiprism graph on  $G \oplus G'$  either by a horizontal or a vertical extension, we obtain another graph of unique RAC combinatorial embedding. In this way, we can define an infinite class of graphs of unique RAC combinatorial embedding. This is summarized in the following theorem.

**Theorem 3.** *There exists a class of graphs of unique RAC combinatorial embedding.*

## 4 The Straight-Line RAC Drawing Problem is NP-Hard

**Theorem 4.** *It is NP-hard to decide whether an input graph admits a straight-line RAC drawing.*

*Proof.* We will reduce the well-known 3-SAT problem to the straight-line RAC drawing problem. In a 3-SAT instance, we are given a formula  $\phi$  in conjunctive normal form with variables  $x_1, x_2, \dots, x_n$  and clauses  $C_1, C_2, \dots, C_m$ , each with three literals. We show how to construct a graph  $G_\phi$  that admits a straight-line RAC drawing  $\Gamma(G_\phi)$  if and only if formula  $\phi$  is satisfiable.

Figure 3 illustrates the gadgets of our construction. Each gray-colored square in these drawings corresponds to an augmented square antiprism graph. Adjacent gray squares form an extension (refer, for example, to the topmost gray squares of Figure 3a, which form a “horizontal” extension). There also exist gray squares that are not adjacent, but connected with edges. The legend in Figure 3 describes how the connections are realized.

The gadget that encodes variable  $x_i$  of formula  $\phi$  is given in Figure 3a. The gadget of variable  $x_i$  consists of a combination of augmented square antiprism



graphs, and, “horizontal” and “vertical” edges, which form a tower, whose RAC drawing has unique combinatorial embedding. One side of the tower accommodates multiple vertices that correspond to literal  $x_i$ , whereas its opposite side accommodates vertices that correspond to literal  $\bar{x}_i$  (refer to vertices  $x_{i,1}, \dots, x_{i,m}$  and  $\bar{x}_{i,1}, \dots, \bar{x}_{i,m}$  in Figure 3a). These vertices are called *variable endpoints*. Then, based on whether on the final drawing the negated vertices will appear to the “left” or to the “right” side of the tower, we will assign a true or a false value to variable  $x_i$ , respectively. Pairs of consecutive endpoints  $x_{i,j}$  and  $x_{i,j+1}$  are separated by a *corridor* (see Figure 3a), which allows perpendicular edges to pass through it (see the bottommost dashed arrow of Figure 3a). Note that this is not possible through a “corridor” formed on a variable endpoint, since there exist four non-parallel edges that “block” any other edge passing through them (see the topmost dashed arrow of Figure 3a). The corridors can have variable height. In the variable gadget of variable  $x_i$ , there are also two vertices (they are drawn as gray circles in Figure 3a), which have degree four. These vertices serve as “connectors” among consecutive variable gadgets, i.e., these vertices should be connected to their corresponding vertices on the variable gadgets of variables  $x_{i-1}$  and  $x_{i+1}$ . Note that the connector vertices of the variable gadgets associated with variables  $x_1$  and  $x_n$  are connected to connectors of the variable gadgets that correspond to variables  $x_2$  and  $x_{n-1}$ , respectively, and to connectors of *dummy variable gadgets*.

Figure 3b illustrates a dummy variable gadget, which (similarly to the variable gadget) consists of a combination of augmented square antiprism graphs, and, “horizontal” and “vertical” edges, which form a tower. Any RAC drawing of this gadget has also unique combinatorial embedding. A dummy variable gadget does not support vertices that correspond to literals. However, it contains connector vertices (they are drawn as gray circles in Figure 3b). In our construction, we use exactly two dummy variable gadgets. The connector vertices of each dummy variable gadget should be connected to their corresponding connector vertices on the variable gadgets associated with variables  $x_1$  and  $x_n$ , respectively.

The gadget that encodes the clauses of formula  $\phi$  is illustrated in Figure 3c and resembles a valve. Let  $C_i = (x_j \vee x_k \vee x_l)$  be a clause of  $\phi$ . As illustrated in Figure 3c, the gadget which corresponds to clause  $C_i$  contains three vertices<sup>1</sup>, say  $x_j$ ,  $x_k$ , and  $x_l$ , such that:  $x_j$  has to be connected to  $x_{j,i}$ ,  $x_k$  to  $x_{k,i}$  and  $x_l$  to  $x_{l,i}$  by paths of length two. These vertices (i.e.,  $x_j$ ,  $x_k$ , and  $x_l$ ), referred to as the *clause endpoints*, encode the literals of each clause. Obviously, if a clause contains a negated literal, it should be connected to the negated endpoint of the corresponding variable gadget. The clause endpoints are incident to a vertex “trapped” within two parallel edges (refer to the bold drawn edges of Figure 3c). Therefore, in a RAC drawing of  $G_\phi$ , only two of them can perpendicularly cross these edges, one from top (*top endpoint*; refer to clause endpoint  $x_l$  of Figure 3c) and one from bottom (*bottom endpoint*; refer to clause endpoint  $x_j$  of Figure 3c). The other one (*right endpoint*; refer to clause endpoint  $x_k$  of

<sup>1</sup> With slight abuse of notation, the same term is used to denote variables of  $\phi$  and vertices of  $G_\phi$ .

Figure 3c) should remain in the interior of the two parallel edges. The one that will remain “trapped” on the final drawing will correspond to the true literal of this clause (see Figure 3).

The gadgets, which correspond to variables and clauses of  $\phi$ , are connected together by the skeleton of graph  $G_\phi$ , which is depicted in Figure 4a. The skeleton consists of two main parts, i.e., one “horizontal” and one “vertical”. The vertical part accommodates the clause gadgets (see Figure 4a). The horizontal part will be used in order to “plug” the variable gadgets. The long edges that perpendicularly cross (refer to the crossing edges slightly above the horizontal part in Figure 4a), imply that the vertical part should be perpendicular to the horizontal part. The horizontal part of the skeleton is separately illustrated in Figure 4b. Observe that it contains one set of horizontal lines.

Figure 5 shows how the variable gadgets are attached to the skeleton. More precisely, this is accomplished by a single edge, which should perpendicularly cross the set of the horizontal edges of the horizontal part. Therefore, each variable gadget is perpendicularly attached to the skeleton, as in Figure 5. Note that each variable gadget should be drawn completely above of these horizontal edges, since otherwise the connections among variable endpoints and clause endpoints would not be feasible. The connector vertices of the dummy variable

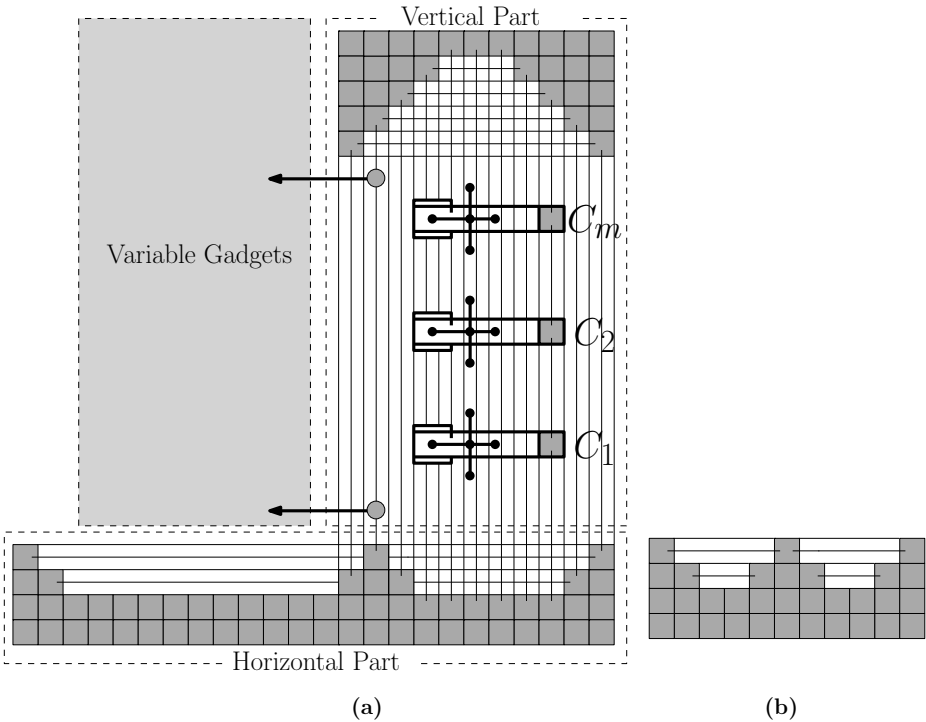


**Fig. 4.** Illustration of the skeleton of the construction

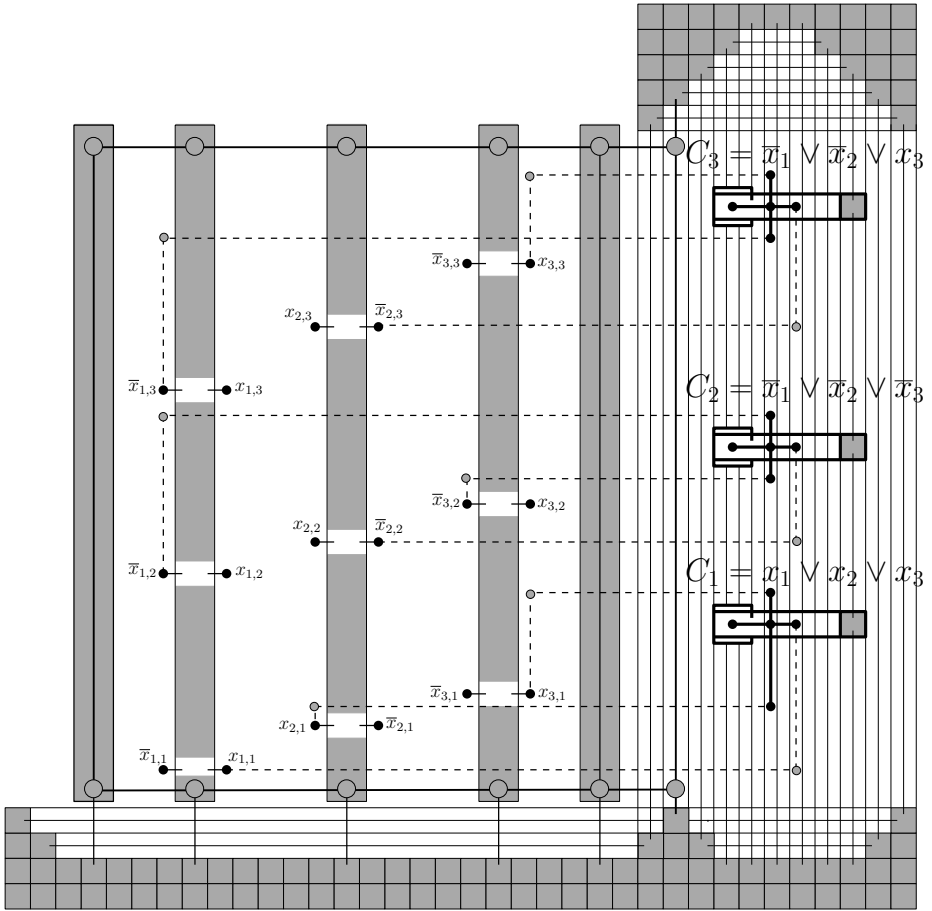


**Fig. 5.** The reduction from 3-SAT to the straight-line RAC drawing problem. The input formula is  $\phi = (x_1 \vee x_2 \vee x_3) \wedge (\bar{x}_1 \vee \bar{x}_2 \vee \bar{x}_3) \wedge (\bar{x}_1 \vee \bar{x}_2 \vee x_3)$ . The drawing corresponds to the truth assignment  $x_1=x_3=\text{true}$ ,  $x_2=\text{false}$ .

gadgets, the variable gadgets and the vertical part of the construction, ensure that the variable gadgets will be parallel to each other (i.e., they are not allowed to bend) and parallel to the vertical part of the construction.

We now proceed to investigate some properties of our construction. Any path of length two that emanates from a top- or bottom-clause endpoint can reach a variable endpoint either on the left or on the right side of its associated variable gadget. The first edge of this path should perpendicularly cross the vertical edges of the vertical part of the construction and pass through some corridors<sup>2</sup>, whereas the second edge will be used to realize the “final” connection with the variable gadget endpoint (see Figure 5). However, the same doesn’t hold for the paths

<sup>2</sup> In Figure 5, the corridors are the gray-colored regions that reside at each variable gadget.

that emanate from a right-clause endpoint. These paths can only reach variable endpoints on the right side of their associated variable gadgets. More precisely, the first edge of the 2-length path should cross one of the two parallel edges (refer to the bold drawn edges of Figure 3c) that “trap” it, whereas the other one should be used to reach (passing through variable corridors) its variable endpoint (see Figure 5).

Our construction ensures that up to translations, rotations and stretchings any RAC drawing of  $G_\phi$  resembles the one of Figure 4. Each tower corresponding to a non-dummy variable gadget of the construction contributes  $O(m)$  time to the total construction time. The towers that correspond to dummy variable gadgets trivially contribute constant time to the total construction time. Therefore, we can construct all towers of variable gadgets in  $O(nm)$  time. The horizontal part needs an extra  $O(n)$  time, whereas the vertical part can be done in  $O(m)$  time. Thus, our construction can be completed in  $O(nm)$  time in total. Assume now that there is a RAC drawing  $\Gamma(G_\phi)$  of  $G_\phi$ . If the negated vertices of the variable gadget that corresponds to  $x_i$ ,  $i = 1, 2, \dots, n$ , lie to the “left” side in  $\Gamma(G_\phi)$ , then variable  $x_i$  is set to true, otherwise  $x_i$  is set to false. We argue that this assignment satisfies  $\phi$ . To realize this, observe that there exist three paths that emanate from each clause gadget. The one that emanates from the right endpoint of each clause gadget can never reach a false value. Therefore, each clause of  $\phi$  must contain at least one true literal, which implies that  $\phi$  is satisfiable.

Conversely, suppose that there is a truth assignment that satisfies  $\phi$ . We proceed to construct a RAC drawing  $\Gamma(G_\phi)$  of  $G_\phi$ , as follows: In the case where, in the truth assignment, variable  $x_i$ ,  $i = 1, 2, \dots, n$  is set to true, we place the negated vertices of the variable gadget that corresponds to  $x_i$ , to its left side in  $\Gamma(G_\phi)$ , otherwise to its right side. Since each clause of  $\phi$  contains at least one true literal, we choose this as the right endpoint of its corresponding clause gadget. As mentioned above, it is always feasible to be connected to its variable gadgets by paths of length two. This completes our proof.  $\square$

## 5 Conclusions

In this paper, we proved that it is  $\mathcal{NP}$ -hard to decide whether a graph admits a straight-line RAC drawing. Didimo et al. [8] proved that it is always feasible to construct a RAC drawing of a given graph with at most three bends per edge. If we permit two bends per edge, does the problem remain  $\mathcal{NP}$ -hard? It is also interesting to continue the study on the interplay between the number of edges and the required area in order to fill the gaps between the known upper and lower bounds.

## References

1. Angelini, P., Cittadini, L., Di Battista, G., Didimo, W., Frati, F., Kaufmann, M., Symvonis, A.: On the perspectives opened by right angle crossing drawings. In: Eppstein, D., Gansner, E.R. (eds.) GD 2009. LNCS, vol. 5849, pp. 21–32. Springer, Heidelberg (2010)

2. Argyriou, E.N., Bekos, M.A., Symvonis, A.: Maximizing the total resolution of graphs. In: 18th International Symposium on Graph Drawing (2010) (to appear)
3. Argyriou, E.N., Bekos, M.A., Symvonis, A.: The straight-line RAC drawing problem is NP-hard. CoRR abs/1009.5227 (2010)
4. Arikushi, K., Fulek, R., Keszegh, B., Moric, F., Toth, C.: Drawing graphs with orthogonal crossings. In: 36th International Workshop on Graph Theoretic Concepts in Computer Science (2010) (to appear)
5. Battista, G.D., Eades, P., Tamassia, R., Tollis, I.G.: Graph Drawing: Algorithms for the Visualization of Graphs. Prentice-Hall, Englewood Cliffs (1999)
6. Bodlaender, H.L., Tel, G.: A note on rectilinearity and angular resolution. *Journal of Graph Algorithms and Applications* 8, 89–94 (2004)
7. Di Giacomo, E., Didimo, W., Liotta, G., Meijer, H.: Area, curve complexity, and crossing resolution of non-planar graph drawings. In: Eppstein, D., Gansner, E.R. (eds.) GD 2009. LNCS, vol. 5849, pp. 15–20. Springer, Heidelberg (2010)
8. Didimo, W., Eades, P., Liotta, G.: Drawing graphs with right angle crossings. In: Dehne, F., Gavrilova, M., Sack, J.-R., Tóth, C.D. (eds.) *Algorithms and Data Structures*. LNCS, vol. 5664, pp. 206–217. Springer, Heidelberg (2009)
9. Didimo, W., Eades, P., Liotta, G.: A characterization of complete bipartite graphs. *Information Processing Letters* 110(16), 687–691 (2010)
10. Dujmovic, V., Gudmundsson, J., Morin, P., Wolle, T.: Notes on large angle crossing graphs. In: 16th Symposium on Computing: the Australasian Theory, pp. 19–24. Australian Computer Society (2010)
11. Formann, M., Hagerup, T., Haralambides, J., Kaufmann, M., Leighton, F., Symvonis, A., Welzl, E., Woeginger, G.: Drawing graphs in the plane with high resolution. *SIAM Journal of Computing* 22(5), 1035–1052 (1993)
12. Garey, M., Johnson, D.: Crossing number is NP-complete. *SIAM Journal of Algebraic Discrete Methods* 4, 312–316 (1983)
13. Garg, A., Tamassia, R.: Planar drawings and angular resolution: Algorithms and bounds (extended abstract). In: 2nd Annual European Symposium on Algorithms, pp. 12–23 (1994)
14. Gutwenger, C., Mutzel, P.: Planar polyline drawings with good angular resolution. In: Whitesides, S.H. (ed.) GD 1998. LNCS, vol. 1547, pp. 167–182. Springer, Heidelberg (1999)
15. Huang, W.: Using eye tracking to investigate graph layout effects. In: Asia-Pacific Symposium on Visualization, pp. 97–100 (2007)
16. Huang, W., Hong, S.-H., Eades, P.: Effects of crossing angles. In: IEEE Pacific Visualization Symposium, pp. 41–46. IEEE, Los Alamitos (2008)
17. Kaufmann, M., Wagner, D. (eds.): *Drawing Graphs*. LNCS, vol. 2025. Springer, Heidelberg (2001)
18. van Kreveld, M.: The quality ratio of RAC drawings and planar drawings of planar graphs. In: 18th International Symposium on Graph Drawing (2010) (to appear)
19. Malitz, S.M., Papakostas, A.: On the angular resolution of planar graphs. In: 24th Annual ACM Symposium on Theory of Computing, pp. 527–538. ACM, New York (1992)
20. Purchase, H.C., Carrington, D.A., Allder, J.-A.: Empirical evaluation of aesthetics-based graph layout. *Empirical Software Engineering* 7(3), 233–255 (2002)